IEEE Access
Multidisciplinary | Rapid Review | Open Access Journal

Received May 16, 2019, accepted July 3, 2019, date of publication July 8, 2019, date of current version July 24, 2019.

Digital Object Identifier 10.1109/ACCESS.2019.2927225

Edge Extraction Based on Memristor Cell Neural Network With Fractional Order Template

CHUNBO XIU[1,2] **AND XIN LI**[1]

[1]School of Electrical Engineering and Automation, Tianjin Polytechnic University, Tianjin 300387, China
[2]Key Laboratory of Advanced Electrical Engineering and Energy Technology, Tianjin Polytechnic University, Tianjin 300387, China

Corresponding author: Chunbo Xiu (xiuchunbo@tjpu.edu.cn)

This work was supported in part by the Natural Science Foundation of Tianjin, China, under Grant 18JCYBJC88300 and Grant 18JCYBJC88400.

ABSTRACT In order to extract more texture and detail information from a given image, a memristor cell neural network is proposed by replacing the state resistances of the neurons as the memristors. The characteristic of memristor could be maintained in the whole information processing of the cell neural network so that the historical state information could be used and the information processing ability of the network could be enhanced. Furthermore, based on the fractional order calculus theory, a fractional order control template is designed for the memristor cell neural network to enhance the middle- and high-frequency information and retain more low-frequency texture information in the image edge extraction. The network could be used to extract edge information from various kinds of images. The simulation results show that the edge images extracted by this method have more complete and clear contour information and more abundant texture detail information. Both the average gradient and the information entropy of the edge images could be significantly improved.

INDEX TERMS Fractional order differential, memristor, cell neural network (CNN), edge extraction.

I. INTRODUCTION

Image edge extraction is one of the key technologies in image processing, which has been widely applied in many fields, such as image segmentation, image compression, image understanding, and so on [1], [2]. Traditional edge extraction methods are based on the edge detection operators, such as Roberts operator, Sobel operator, Prewitt operator, Laplacian operator, Log operator, Canny operator and so on. These methods are easy to implement, but poor universality. Cellular neural network (CNN) [3]–[5], as a kind of dynamic neural network, could also be used to extract the image edge. It has the local interconnection structure and the high-speed parallel processing ability. The network could converge to the expected stable state according to its own dynamic characteristics in the case of reasonable design of network structure. It shows good application performance in many fields such as image denoising, edge extraction and associative memory [6]–[8].

Cellular neural network usually adopts the local interconnection structure between the central cell and its neighborhood cells, and the communication between the central cell and its neighborhood cells could be implemented by a multiplier. However, when the image size is large, the number of cells would also increases, and the circuit structure of cellular neural network would become complex, which makes it inconvenient to update the weight template [9]–[11]. Since the physical model of memristor is developed in HP laboratory [12], the study on the memristor cell neural network (MCNN) has been recognized as a new research hotspot in the field of neural network. The memristor has the natural memory characteristic, so the information processing ability of memristor cellular neural network could be further improved [13], [14]. At the present research stage, the memristor is often used as the connection weight of the neural network. In this way, the flexible weight adjustment of the neural network could be easily implemented by the memristor [15], [16]. Generally, the work procedure of memristor cellular neural networks could be divided into two stages: the weight adjustment stage and the information processing stage. In the stage of weight adjustment, the resistance of the memristor is changed by controlling its electrified time. Thus, the weight template of the memristor cellular neural network could be changed and the network is set as the

The associate editor coordinating the review of this manuscript and approving it for publication was Choon Ki Ahn.

desired function. Then, in the information processing stage, the weights of the network are fixed, and the network carries out the corresponding information processing tasks in the same way as the traditional cellular neural network. However, in this way, the memristor only plays the role of the weight adjustment, and the memory characteristics of memristor are not used in the whole information processing. Therefore, the performance of MCNN is the same with that of the traditional cellular neural network.

Cellular neural network, as a dynamic system, would converge to a stable state through a transition process. If the memristor memory characteristic could be integrated into the information processing, it would enhance the utilization rate of historical information, improve the memory ability of the network, and ameliorate the application performance of the network.

Besides, the effect of CNN in image edge extraction is closely related to the design of the weight templates which could be commonly designed by the constraint analysis method or the learning method. The learning method train the weight template by the given or ideal image samples [17]–[19]. Instead, the constraint analysis method directly design the weight template according to the task without the sample space [20], [21]. However, the edge extraction template based on the integer order calculus could only enhance the high-frequency information in the image, and greatly suppress the middle-frequency and the low-frequency information. Therefore, some blurry texture and detail information would be lost during the image edge extraction.

It is well-known that fractional order calculus is an extension of integer order calculus. Compared with integer order calculus, fractional order differential could not only dramatically enhance the high-frequency information, but also heighten the middle-frequency information and retain the low-frequency information in nonlinear [22]–[24]. Therefore, fractional calculus theory could be applied to improve the image processing performance [25]–[29]. Such as, the restoring and maintaining the edges and textural details capability of the fractional-order image restoration algorithm is superior to that of the integer-order image restoration algorithm [30]. The image denoising method based on fractional calculus operator could not only preserve more image edges and texture information, but also get a better visual effect [31]. Contrast Enhancement method based on the fractional order differential could preserve edges and textural details than that based on the integer order differential [32]. Above all, the image processing methods based on fractional calculus theory could retain more texture and detail information of the middle-frequency and the low-frequency.

Therefore, in order to improve the edge detection performance, a novel memristor cell neural network model is proposed. A fractional order edge detection control template is designed to reserve the middle-frequency and the low-frequency information in the image, and the memristor memory characteristic always plays the role to enhance the utilization ratio of information in the whole process of the information processing. Thus, more fine texture details could be extracted from the original image.

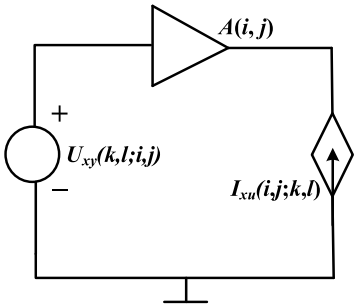

FIGURE 1. The model of the voltage controlled current source in CNN.

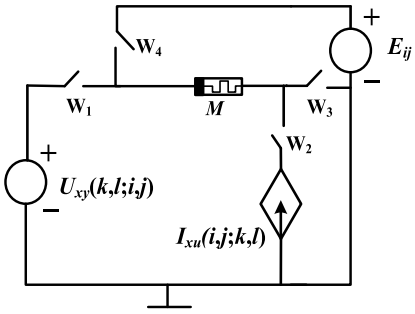

FIGURE 2. The model of voltage-controlled current source in MCNN.

II. MEMRISTOR CELLULAR NEURAL NETWORK

The connection weights of the traditional cellular neural network could be implemented by multiplier. The model of the voltage controlled current source in the network is shown in Figure 1.

From Figure 1, the connection weight template of CNN is fixed. If the connection weights need to be changed, the network must be reconstructed. Therefore, the network is lack of flexibility.

The resistance of memristor could be changed with its applied voltage or current. When different excitations were applied to the memristor, the memristor would exhibit different hysteretic memory characteristics. The controllability of the memristor resistance could be used to adjust flexibly the connection weights of CNN in hardware.

The structure of voltage-controlled current source in memristor cell neural network is given in Figure 2.

In Figure 2, when the W_1 and W_2 are opened and W_3 and W_4 are closed, the memristor weight M could be adjusted. At this time, the input excitation of the memristor would be larger than its adjustment threshold, the resistance of the memristor could be changed by controlling the time of the input excitation. That is, the resistance of the memristor could be changed by the applied voltage. In the working stage of the network, W_1 and W_2 are closed, W_3 and W_4 are opened, and the memristor weight M would be

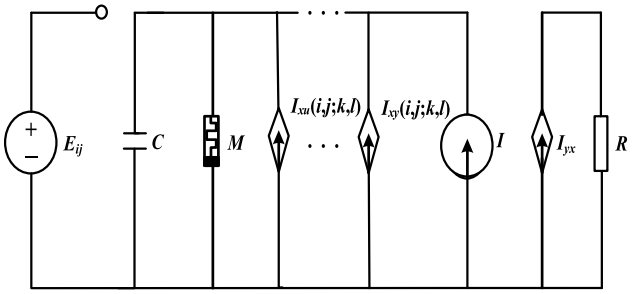

FIGURE 3. The equivalent circuit of the memristor neuron x_{ij}.

connected into the CNN. At this time, the input excitation on the memristor is less than its adjustment threshold, and the resistance of the memristor could not be changed. The memristor value would be fixed in the network in the information processing.

Although the weights could be flexibly and conveniently adjusted in the way above, the memristor characteristic would disappear in the working stage. The network could only work as the same way of the traditional cellular neural network, and the information processing performance could not be improved significantly.

In order to take full advantage of the memristor memory characteristics to improve the information processing performance, a new memristor cell neural network is constructed by keeping the memristor memory characteristic in the whole process of information processing. The equivalent circuit of the neuron is shown in Figure 3.

In Figure 3, the state resistance of the central cell is designed as a memristor, and the memristor value would be changed according to the applied voltage. The state equation of memristor cellular neural networks could be described as:

$$\frac{dx_{ij}(t)}{dt} = -M(x_{ij}(t)) + \sum_{C(k,l)} (a_{ij,kl}y_{kl} + b_{ij,kl}u_{kl}(t)) + I \quad (1)$$

$$y_{ij} = \frac{1}{2}(|x_{ij}(t)+1| - |x_{ij}(t)-1|) \quad (2)$$

The feedback template a_{ij}, kl indicates the effect of the output y_{kl} of the neighboring cells on the central cells C(i, j). The control template b_{ij}, kl indicates the effect of the input $u_{kl}(t)$ of the neighboring cells on the central cells C(i, j). The function y_{ij} is the output of the central cells C(i, j).

$M(t)$ is the memristor value which is based on the boundary migration model given in Reference[16] as:

$$M(t) = R_{\mathrm{ON}}\frac{w}{D} + R_{\mathrm{OFF}}(1 - \frac{w}{D}) \quad (3)$$

where, D represents the thickness of the thin film between the electrodes, and w represents the width of the high conductivity doped region, and w is between 0 and D. When $w = 0$, the dielectric material of the memristor is entirely composed of undoped region, and the memristor value reaches the maximum R_{OFF}, that is,

$$M(t) = R_{\mathrm{OFF}} \quad (4)$$

When $w = D$, the dielectric material of the memristor is entirely composed of doped region, and the memristor value reaches the minimum R_{ON}, that is,

$$M(t) = R_{\mathrm{ON}} \quad (5)$$

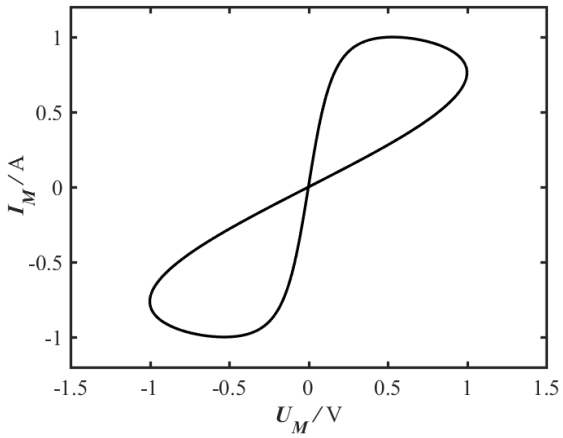

FIGURE 4. Volt-ampere characteristics of the memristor.

When different excitations are applied to the memristor, the memristor would exhibit different characteristics. For instance, Figure 4 gives the volt-ampere characteristics of the memristor.

From Figure 4, the memristor value is related to its applied voltage process. For the same applied voltage, the memristor value could be different due to different historical states. Therefore, the historical information could be memorized in the memristor. Therefore, the characteristic of memristor could be maintained in the whole information processing of CNN, so that the historical state information could be used, and the information processing ability of the network could be enhanced.

When the MCNN above is used to extract the image edge, the state of the network can automatically converge to a steady state according to the dynamics characteristics of the network. In this way, the historical state information of the neurons could play a positive role in extracting the image edge.

The image edge extraction performance of MCNN is related closely to the control template $\boldsymbol{B}$. The traditional edge extraction template based on the integer calculus could only boost the high-frequency information, and suppress the middle and low frequency information, which cause the loss of some detail information. The existing fractional order calculus theory shows that the fractional order differential could not only boost the high frequency information, but also enhance the middle frequency information and nonlinearly retain the low frequency information. For this

reason, a fractional order differential edge extraction template is designed for MCNN to improve the edge detection performance.

III. FRACTIONAL ORDER CONTROL TEMPLATE

The sizes of the feedback template $\boldsymbol{A}$ and the control template $\boldsymbol{B}$ determine the receptive filed of the neurons and the computation cost of the network. When the feedback template and the control template of CNN are chosen as the size of 3×3, the forms of the network templates, $\boldsymbol{A}$, $\boldsymbol{B}$, and the threshold I, could be designed as:

$$\boldsymbol{A} = \begin{bmatrix} 0 & 0 & 0 \\ 0 & a & 0 \\ 0 & 0 & 0 \end{bmatrix} \quad \boldsymbol{B} = \begin{bmatrix} b_1 & b_1 & b_1 \\ b_1 & b_0 & b_1 \\ b_1 & b_1 & b_1 \end{bmatrix} \quad I < 0 \tag{6}$$

In Eq. (6), the parameters, a, b_0, b_1 and I, are the main parameters of the network. The parameter a should meet the constraint condition, $a > 1/R_{\mathrm{OFF}}$, to make the network converge to the steady binary output state [9]. Besides, the parameters, b_0, b_1 and I, should meet the following constraint conditions to make the network perform the edge detection [9]:

$$|b_0 + 8b_1| < |I| < |b_0 + 6b_1| \tag{7}$$

The constraint conditions above are just the sufficient conditions of the image edge extraction. In order to retaining more middle and low frequency information in the edge image, a fractional order differential edge extraction template is constructed under constrain conditions above for MCNN. Thus, more texture and detail information in the middle or the low frequency domain would be retained in the edge image.

For now, there are three common definitions of the fractional order calculus: Riemann-Liouville (R-L) fractional calculus, Grünwald-Letnikov (G-L) fractional calculus and Caputo fractional calculus. The numerical calculation based on R-L fractional order differential definition or G-L fractional order differential definition could be transformed into convolution integral calculation, so R-L definition or G-L definition is best applied to the signal processing field. By contrast, Caputo fractional order differential definition is best applied to the initial boundary value problem of the fractional differential equation. Moreover, R-L fractional order differential definition and G-L fractional order differential definition are equivalent [27]. Above all, for the image edge extraction problem, R-L fractional order differential definition is used to design the control template.

For a function $f(t)$, its R-L fractional order differential is defined as:

$${}_aD_t^{\alpha} f(t) = \frac{1}{\Gamma(n-\alpha)} \frac{d^n}{dt^n} \int_a^t (t-\tau)^{n-\alpha-1} f(\tau) d\tau \tag{8}$$

where, $\Gamma(\cdot)$ is the second type of Euler integral-Gamma function. In the fractional order differential operator ${}_aD_t^{\alpha}$, a and t are separately the upper and the lower bounds of the integral, and α is the differential order, where, $0 \le n-1 \le \alpha \le n$ and $t > a$.

When $f(t) \equiv c$, where c is a constant, for $0 < \alpha < 1$,

$${}_aD_t^{\alpha} c = \frac{c(t-a)^{-\alpha}}{\Gamma(1-\alpha)} \neq 0 \tag{9}$$

According to Eq. (9), for a constant or no fluctuation function, its fractional order differential is not zero. That is, the fractional order differential could extract some tiny change information. For an image, the fractional order differential is high sensitive to the slight fluctuation of the gray value. Therefore, the fractional order differential edge detection template could be designed to extract some indistinctive texture information from the image.

For the discrete pixels in an image, the continuous fractional order differential operator must be discretized. Set $a = 0$ and the step $h = 1$. The interval [0,t] is divided into m equal pieces and t is an integer. Thus, $m = (t\text{-}a)/h = t$. Suppose $\tau = 0, 1, 2, \ldots, m$.

According to the discrete Fourier transform, the fractional order differential operator could be discretized as:

$$\begin{aligned} {}_aD_t^{\alpha} f(t) &= \frac{1}{\Gamma(n-\alpha)} \frac{d^n}{dt^n} \int_a^t (t-\tau)^{n-\alpha-1} f(\tau) d\tau \\ &\cong \frac{1}{\Gamma(n-\alpha)} \sum_{i=0}^{m-1} (n-\alpha-1)(n-\alpha-2) \\ &\quad \cdots (-\alpha)(t-i)^{-\alpha-1} f(i) \\ &= \frac{1}{\Gamma(n-\alpha)} (n-\alpha-1)(n-\alpha-2) \\ &\quad \cdots (-\alpha)[(1)^{-\alpha-1} f(t-1) \\ &\quad + (2)^{-\alpha-1} f(t-2) + \cdots \\ &\quad + (t-1)^{-\alpha-1} f(1) + (t-0)^{-\alpha-1} f(0)] \end{aligned} \tag{10}$$

According to Eq. (10), a fractional order differential edge extraction template could be designed for the image with the size $M \times N$. The template is designed to be isotropic. b_i is the coefficient in the i-th layer around the central point. Thus, according to Eq. (11), the coefficient b_i could be described as:

$$b_i = \frac{1}{\Gamma(n-\alpha)} (n-\alpha-1)(n-\alpha-2) \cdots (-\alpha)(2i)^{-\alpha-1} \tag{11}$$

If set $0 < \alpha < 1$, then $n = 1$. Thus,

$$b_i = \frac{1}{\Gamma(1-\alpha)} (-\alpha)(2i)^{-\alpha-1} \tag{12}$$

Fractional order differential edge detection template coefficients are arranged in layers. To ensure the sum of template coefficients to be zero, b_0 is set as:

$$b_0 = -8 \sum_{i=1}^{n} i \cdot b_i \tag{13}$$

For instance, when $\alpha = 0.5$, the coefficients could be calculated as: $b_1 = -0.0997$ and $b_0 = 0.7976$. Thus, the control template $\boldsymbol{B}$ with the size of 3×3 could be designed

as:

$$\boldsymbol{B} = \begin{bmatrix} b_1 & b_1 & b_1 \\ b_1 & b_0 & b_1 \\ b_1 & b_1 & b_1 \end{bmatrix} = \begin{bmatrix} -0.0997 & -0.0997 & -0.0997 \\ -0.0997 & 0.7976 & -0.0997 \\ -0.0997 & -0.0997 & -0.0997 \end{bmatrix} \tag{14}$$

It can be verified that the parameters meet the constraint conditions in Eq. (7) in case of $0> \ I \ > -0.1994$. For instance, the parameter I could be set as -0.03. Therefore, MCNN based on the fractional order template (MCNN-FOT) above could be used to extract the image edge. The edge extraction process based on MCNN-FOT could be described as:

Step 1: Memristor cellular neural networks is designed according to the size of the image. The number of neurons is equal to the number of the pixels in the image.

Step 2: Design off-line the feedback template, the control template and threshold according to the constraint conditions.

Step 3: Input the image to the MCNN-FOT, and iterate the network until the network converges to a stable state.

Step 4: Output the stable state which is just the edge extraction result.

Both the feedback template and the control template are designed off-line, so the online calculation cost is not increased. That is, the calculation complexity of MCNN-FOT is equivalent to that of CNN.

IV. EXPERIMENTAL RESULTS AND ANALYSIS

A. PARAMETER ANALYSIS

Some key parameters in MCNN-FOT play the important roles in the process of the edge extraction. Therefore, the experiment analysis is performed to determine the optimal parameters.

According to Eq. (12), the control template of the MCNN-FOT is determined by fractional order α. That is, fractional order α directly impacts on the edge extraction results. Therefore, the MCNN-FOT with the different fractional order template is applied to extract the image edge to show the role of the parameter.

The average gradient G and the information entropy H, which are the most common assessment criteria for the edge extraction, are used to evaluate the edge extraction performance.

The average gradient G is defined as:

$$G = \frac{1}{(M-1)(N-1)} \sum_{i=1}^{M-1} \sum_{j=1}^{N-1} \left[\frac{1}{2} \left(F_{i,j} - F_{i+1,j} \right)^2 + \frac{1}{2} \left(F_{i,j} - F_{i,j+1} \right)^2 \right]^{\frac{1}{2}} \tag{15}$$

where, F_i, j represents the gray value of the pixel in the i-th row and the j-th column in the image. $M \times N$ is the size of the image. The bigger the average gradient is, the more edge information the image contains.

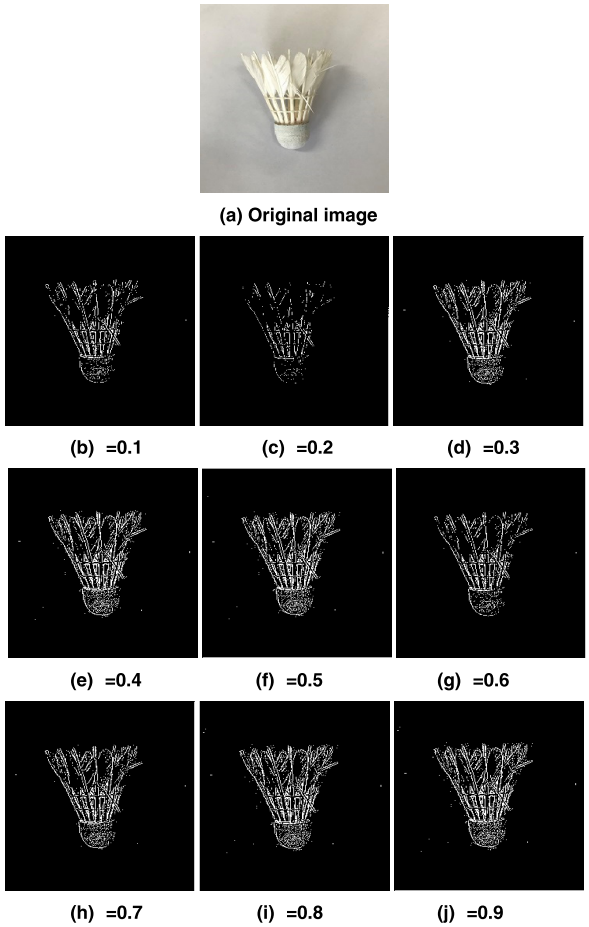

FIGURE 5. The edge detection results with the different fractional order.

The information entropy H is defined as:

$$H = -\sum_{i=1}^{n} p_i \log p_i \tag{16}$$

where, p_i is the proportion of the gray level i. Similarly, the bigger the information entropy is, the more edge information the edge image contains.

The original image is an actual image in which a white badminton in the background with the similar color. The badminton in the image has much edge and texture information. When $I = -0.03$, the edge extraction results are shown in Figure 5.

From Figure 5, intuitively, the edge extraction results with $\alpha \ >0.4$ are similar and the main texture and detail features could be extracted. The average gradient G and the information entropy H of the detection results above are shown in Figure 6 and Figure 7.

From Figure 6 and Figure 7, when $\alpha = 0.5$, both the average gradient and the information entropy would be maximum, which means more texture and detail features could be extracted.

The threshold I is the other key parameter which affects the edge extraction results. When $\alpha = 0.5$, the tendencies of the

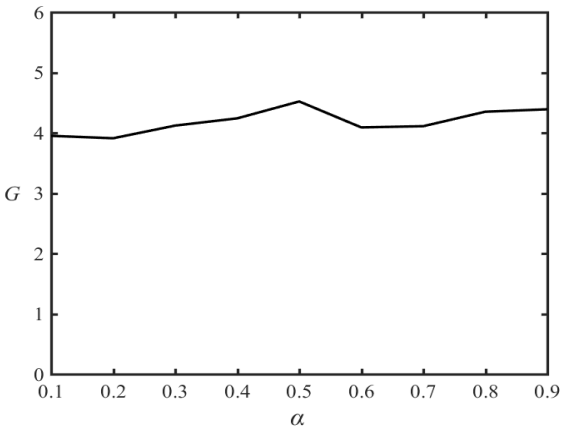

FIGURE 6. The average gradient of the edge detection results.

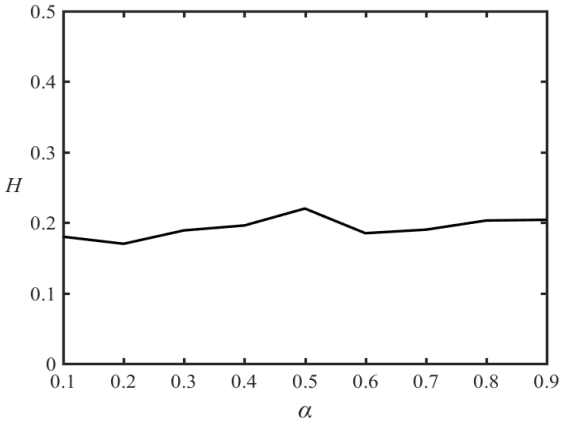

FIGURE 7. The information entropy of the edge detection results.

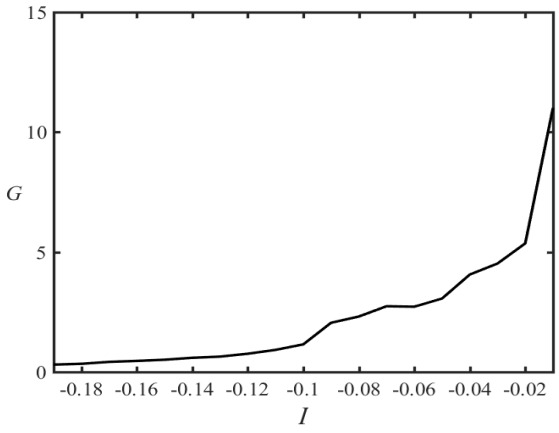

FIGURE 8. The average gradient of the edge detection results.

average gradient G and the information entropy H with the change of the threshold I are shown in Figure 8 and Figure 9.

From Figure 8 and Figure 9, the smaller the absolute value of the threshold I, the bigger the average gradient G and the information entropy H. Figure 10 show the edge extraction results with the different parameter I.

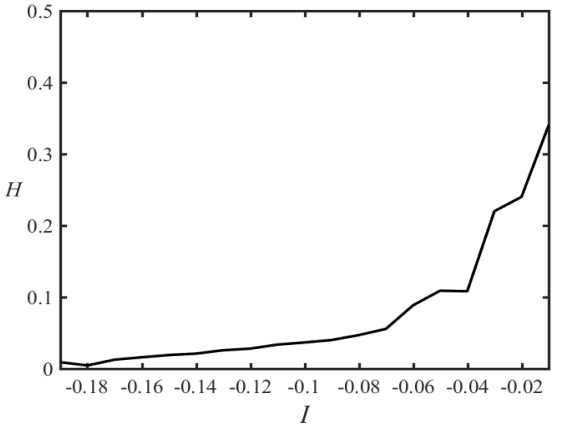

FIGURE 9. The information entropy of the edge detection results.

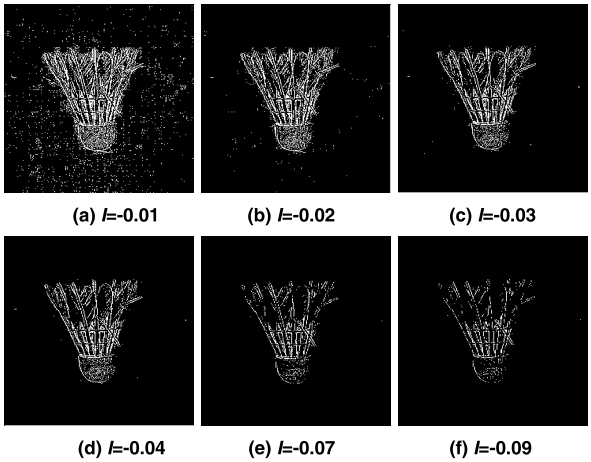

FIGURE 10. The edge detection results with the 3 × 3 template and the different parameter I.

From Figure 10, the threshold just simply determines the number of the edge points. That is, the smaller the absolute value of the threshold, the more noise points obtained in the edge image. Otherwise, the bigger the absolute value of the threshold, the less edge points. By comprehensive consideration, the threshold I is set as -0.03.

Furthermore, the size of the template also affects the network performance. The large size template could make the neuron have a big receptive field which helps to improve the edge extraction results but also increase the computational cost. Figure 11 and Figure 12 are the comparison results of the different template sizes 3×3 and 5×5.

For the different parameter I, the edge extraction results obtained MCNN-FOT with the template size 5×5 are shown in Figure 13.

From Figure 10 to Figure 13, the edge extraction results based on the 5×5 template are better than those based on the 3×3 template. However, the connection number of one neuron would be increased from 9 to 25, which would cause more complex structure and more extra calculation burden.

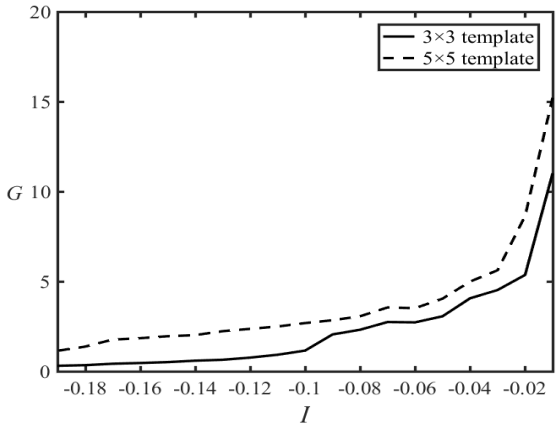

FIGURE 11. The average gradient of the different template sizes 3 × 3 and 5 × 5.

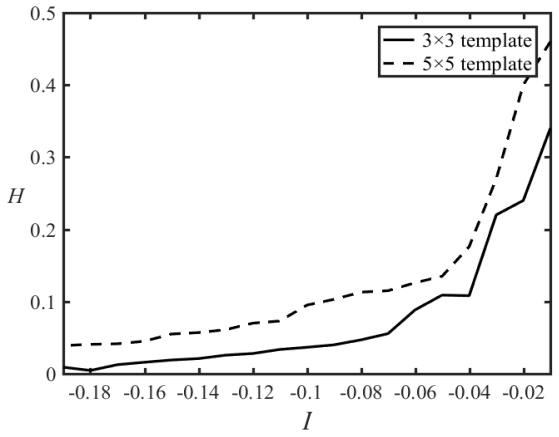

FIGURE 12. The information entropy of the different template sizes 3 × 3 and 5 × 5.

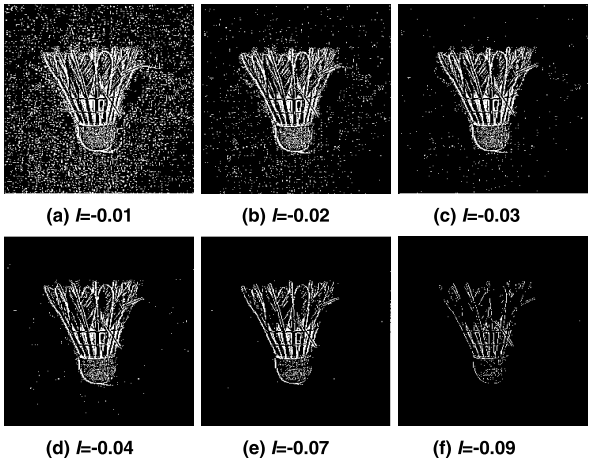

FIGURE 13. The edge detection results with the 5 × 5 template and the different parameter *I*.

Therefore, the 3×3 template is used in MCNN-FOT to extract the image edge.

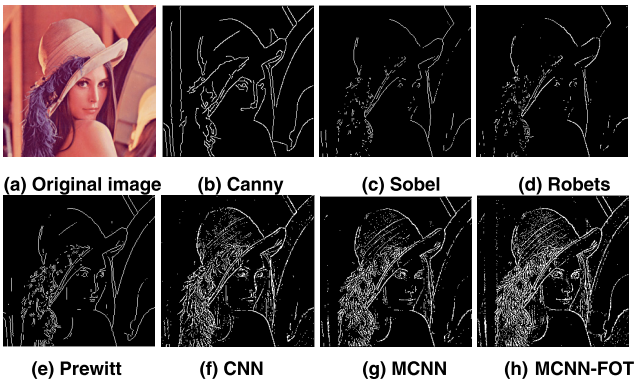

FIGURE 14. Edge detection results of Lena image.

B. THE COMPARISON RESULTS

Based on the parameters above, MCNN-FOT is used to extract the edge from the images with the different characteristics, and the edge extraction results are compared with other methods based on CNN, MCNN, Canny Operator, Sobel Operator, Roberts Operator and Prewitt Operator. Especially, MCNN is the memristors cell neural network without the fractional control template, and MCNN-FOT is the memristors cell neural network with the fractional control template.

1) EDGE EXTRACTION FOR THE DISTINCT OUTLINE IMAGE

The edge of Lena image which has the distinct outline is extracted by the methods above. The extraction results are shown in Figure 14.

Lena image is clear and its main contour edge is easy to extract. From Figure 14, the methods based on the operators could only extract the main edge contours. Much texture and detail information in the low and medium frequency is lost. Instead, the method based on the CNN could extract more texture and detail information. From this aspect, the edge extraction effect of CNN is obviously better than that of the methods based on the detection operators. For instance, the detailed information such as Lena's hat and hair could be extracted. However, some detail information is still lost. For instance, the edge information in the mirror could not be extract entirely. Especially, the upturned mouth is wrongly detected as the downturned mouth. By contrast, MCNN could improve the edge extraction performance because more historical information of the neurons could be utilized in edge extraction process. For instance, the shape of the mouth could be extract correctly. Furthermore, MCNN-FOT could extract more edge information by retaining the low frequency information and enhance the middle-high frequency information. Therefore, the edge information could be extracted more completely and continuously.

2) EDGE EXTRACTION FOR THE GRAY IMAGE

The gray image, Cameraman, has abundant edge information in the foreground and the background. The edge extraction results of the Cameraman image are shown in Figure 15.

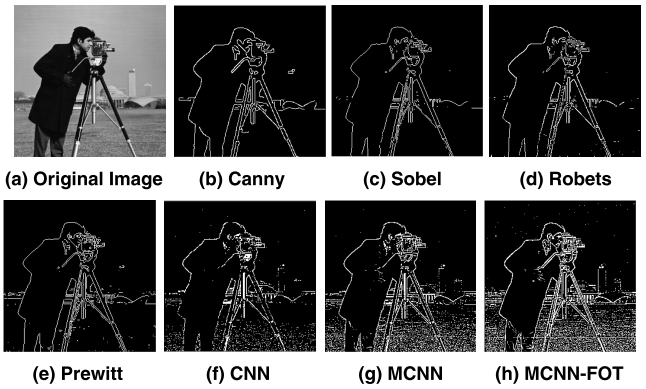

FIGURE 15. Edge detection results of Cameraman image.

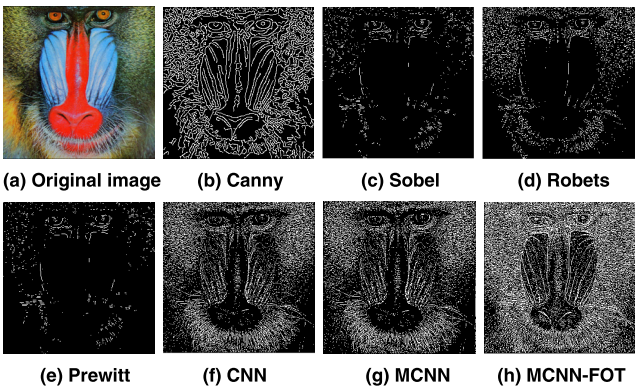

FIGURE 16. Edge detection results of Baboon image.

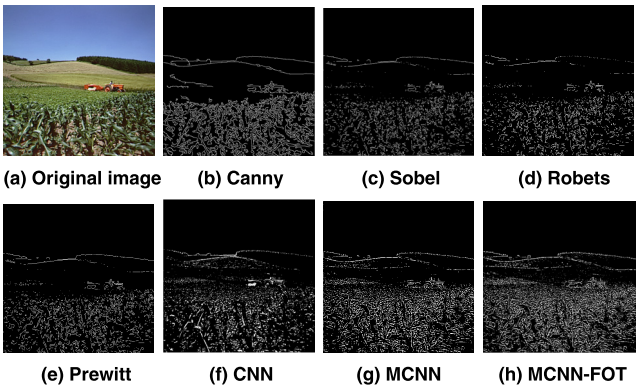

FIGURE 17. Edge detection results of Cornfield image.

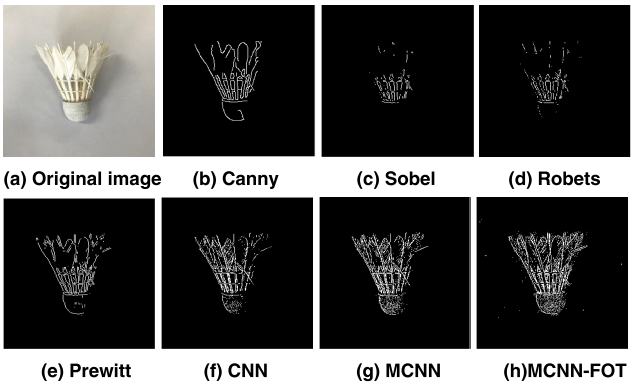

FIGURE 18. Edge detection results of the actual image.

From Figure 15, only approximate contour of Cameraman image could be roughly extracted by the methods based on the edge detection operators. The edge information of the building in the background is almost lost. The integrity contour of Cameraman image could be extracted by CNN. However, the detail information on the camera is still not abundant enough, and the edge of the building is also discontinuous. Comparatively, MCNN has better edge extraction performance than CNN. MCNN could extract the more detail information from the camera in the foreground and the building in the background. Besides, the middle and low frequency edge information of the water ripples in the image could also be extracted precisely by MCNN-FOT.

3) EDGE EXTRACTION FOR THE OBSCURE IMAGE

The obscure Baboon image has much weak whisker texture, and it is difficult to detect the texture detail feature. The edge detection results of Baboon image are shown in Figure 16.

From Figure 16, the edge of this image could not be detected completely by the detection operators, and only part of the edge information could be extracted. The contour of this image extracted by CNN is clearer and the details are more abundant. MCNN could extract more the details of the facial beard and hair, and MCNN-FOT could extract more complete and more continuous contour than CNN and MCNN.

4) EDGE EXTRACTION FOR THE LONG TAKE IMAGE

The Cornfield image contains large number of edge information separately in the close, medium and long shot. The edge detection results of the Cornfield image are shown in Figure 17.

From Figure 17, the edge information of this image could not be extracted completely and continuously by detection operators as well. The edge extraction effect of CNN could be improved, but the vehicles in the medium shot could only be detected as a bright region, so that the actual edge features are not really obtained. MCNN could completely extract the edge contour of crops in close shot, and the edges of vehicles in the medium shot and trees in the long shot could also be detected clearly. MCNN-FOT could extract more middle and low frequency edge information hidden in the cornfield, so the performance of the edge extraction could be improved further.

5) EDGE EXTRACTION FOR THE FINE TEXTURAL IMAGE

The edge extraction results of the actual badminton image are shown in Figure 18.

From Figure 18, the detection results obtained by the methods based on the detection operators are incomplete. CNN could extract most of texture information but the edge information on the right is lost badly. In contrast, MCNN

TABLE 1. The average gradient and the information entropy of the edge image.

Image	Criteria	Canny	Sobel	Roberts	Prewitt	CNN	MCNN	MCNN-FOT
Lena	G	13.24	7.16	7.25	15.13	24.29	29.80	33.65
	H	0.45	0.20	0.17	0.36	0.46	0.57	0.71
Cameraman	G	5.05	4.64	3.50	5.08	8.64	13.83	19.35
	H	0.18	0.22	0.13	0.23	0.28	0.35	0.47
Baboon	G	60.90	15.05	34.11	10.50	75.09	89.6	101.12
	H	0.78	0.34	0.55	0.18	0.82	0.91	0.98
Cornfield	G	19.33	13.36	8.09	11.81	14.28	20.81	27.20
	H	0.69	0.47	0.35	0.32	0.75	0.81	0.86
Badminton	G	1.71	1.01	2.09	3.06	3.60	3.94	4.49
	H	0.08	0.03	0.14	0.18	0.19	0.20	0.21

could extract more texture information than CNN. And more detailed information of the feather texture could be retained by MCNN-FOT.

C. PERFORMANCE ANALYSIS

The performances of the edge extraction results above are shown in TABLE 1.

From TABLE 1, the edge detection operators could only detect the general outline, and a large amount of middle and low frequency information is omitted, so the average gradient and the information entropy are low. In contrast, cellular neural network (CNN) has the better edge detection ability, so both the average gradient and the information entropy could be enhanced. Furthermore, the MCNN could increase the information utilization rate according to the history states of neurons, so more texture detail information could be extracted from the image, and both the average gradient and the information entropy are higher than CNN. MCNN-FOT could heighten the middle-frequency information and retain more low-frequency information, so the average gradient and the information entropy of the edge images extracted by MCNN-FOT are highest.

Furthermore, MCNN has the same structure as CNN, so both of them have the similar convergence performance. Besides, the fractional order differential control template of MCNN-FOT is designed off-line. Therefore, the computational online complexity of MCNN-FOT is also the same as that of CNN. That is, compared with the complexity of CNN, the complexity of MCNN-FOT is not increased.

V. CONCLUSION

In this paper, the model of memristor cellular neural network based on fractional order control template is constructed. The state resistance of neuron is replaced by memristor. Thus, in the process of information processing, the memristor value could be changed with its state voltage. In this way, the information utilization rate could be enhanced, and the performance of the network could be improved. Fractional order template could heighten the middle-frequency information and retain more low-frequency information during the edge extraction. Therefore, the edge contour of image could be continuously and completely detected by the network. Both the average gradient and the information entropy of the edge image obtained by the proposed method are higher than those of other methods.

REFERENCES

[1] E. Hait and G. Gilboa, "Spectral total-variation local scale signatures for image manipulation and fusion," *IEEE Trans. Image Process.*, vol. 28, no. 2, pp. 880–895, Feb. 2019.
[2] M. Seyedhosseini and T. Tasdizen, "Semantic image segmentation with contextual hierarchical models," *IEEE Trans. Pattern Anal. Mach. Intell.*, vol. 38, no. 5, pp. 951–964, Apr. 2016.
[3] T. Matsubara and H. Torikai, "An asynchronous recurrent network of cellular automaton-based neurons and its reproduction of spiking neural network activities," *IEEE Trans. Neural Netw. Learn. Syst.*, vol. 27, no. 4, pp. 836–852, Apr. 2016.
[4] J. C. Chedjou and K. Kyamakya, "A universal concept based on cellular neural networks for ultrafast and flexible solving of differential equations," *IEEE Trans. Neural Netw. Learn. Syst.*, vol. 26, no. 4, pp. 749–762, Apr. 2015.
[5] C. Pan and A. Naeemi, "A proposal for energy-efficient cellular neural network based on spintronic devices," *IEEE Trans. Nanotechnol.*, vol. 15, no. 5, pp. 820–827, Sep. 2016.

[6] D. R. Nayak, R. Dash, B. Majhi, and J. Mohammed, "Non-linear cellular automata based edge detector for optical character images," *Simulation*, vol. 92, no. 9, pp. 849–859, Sep. 2016.
[7] N. Zeng, Z. Wang, B. Zineddin, Y. Li, M. Du, L. Xiao, X. Liu, and T. Young, "Image-based quantitative analysis of gold immunochromatographic strip via cellular neural network approach," *IEEE Trans. Med. Imag.*, vol. 33, no. 5, pp. 1129–1136, May 2014.
[8] J. Müller, R. Wittig, J. Müller, and R. Tetzlaff, "An improved cellular nonlinear network architecture for binary and grayscale image processing," *IEEE Trans. Circuits Syst., II, Exp. Briefs*, vol. 65, no. 8, pp. 1084–1088, Aug. 2018.
[9] L. O. Chua and L. Yang, "Cellular neural networks: Applications," *IEEE Trans. Circuits Syst.*, vol. CAS-35, no. 10, pp. 1273–1290, Oct. 1988.
[10] A. R. Trivedi and S. Mukhopadhyay, "Potential of ultralow-power cellular neural image processing with Si/Ge tunnel FET," *IEEE Trans. Nanotechnol.*, vol. 13, no. 4, pp. 627–629, Jul. 2014.
[11] J. Kung, D. Kim, and S. Mukhopadhyay, "Adaptive precision cellular nonlinear network," *IEEE Trans. Very Large Scale Integr. (VLSI) Syst.*, vol. 26, no. 5, pp. 841–854, May 2018.
[12] D. B. Strukov, G. S. Snider, D. R. Stewart, and R. S. Williams, "The missing memristor found," *Nature*, vol. 453, pp. 80–83, May 2008.
[13] S. Duan, X. Hu, Z. Dong, L. Wang, and P. Mazumder, "Memristor-based cellular nonlinear/neural network: Design, analysis, and applications," *IEEE Trans. Neural Netw. Learn. Syst.*, vol. 26, no. 6, pp. 1202–1213, Jun. 2015.
[14] X. Zhang and W. Jiang, "Construction of flux-controlled memristor and circuit simulation based on smooth cellular neural networks module," *IET Circuits, Devices Syst.*, vol. 12, no. 3, pp. 263–270, May 2018.
[15] E. Bilotta, P. Pantano, and S. Vena, "Speeding up cellular neural network processing ability by embodying memristors," *IEEE Trans. Neural Netw. Learn. Syst.*, vol. 28, no. 5, pp. 1228–1232, May 2017.
[16] X. Hu, G. Feng, S. Duan, and L. Liu, "A memristive multilayer cellular neural network with applications to image processing," *IEEE Trans. Neural Netw. Learn. Syst.*, vol. 28, no. 8, pp. 1889–1901, Aug. 2017.
[17] J. Li and Z. Peng, "Multi-source image fusion algorithm based on cellular neural networks with genetic algorithm," *Optik*, vol. 126, no. 24, pp. 5230–5236, Dec. 2015.
[18] N. Ben Rached, H. Ghazzai, A. Kadri, and M.-S. Alouini, "A time-varied probabilistic on/off switching algorithm for cellular networks," *IEEE Commun. Lett.*, vol. 22, no. 3, pp. 634–637, Mar. 2018.
[19] S. M. S. Tanzil, W. Hoiles, and V. Krishnamurthy, "Adaptive scheme for caching YouTube content in a cellular network: Machine learning approach," *IEEE Access*, vol. 5, pp. 5870–5881, 2017.
[20] M. Zheng, L. Li, H. Peng, J. Xiao, Y. Yang, and Y. Zhang, "Fixed-time synchronization of memristive fuzzy BAM cellular neural networks with time-varying delays based on feedback controllers," *IEEE Access*, vol. 6, pp. 12085–12102, 2018.
[21] J. Müller, J. Müller, R. Braunschweig, and R. Tetzlaff, "A cellular network architecture with polynomial weight functions," *IEEE Trans. Very Large Scale Integr. (VLSI) Syst.*, vol. 24, no. 1, pp. 353–357, Jan. 2016.
[22] D. Wei, "Image super-resolution reconstruction using the high-order derivative interpolation associated with fractional filter functions," *IET Signal Process.*, vol. 10, no. 9, pp. 1052–1061, Dec. 2016.
[23] Y. Wang, Y. Shao, Z. Gui, Q. Zhang, L. Yao, and Y. Liu, "A novel fractional-order differentiation model for low-dose CT image processing," *IEEE Access*, vol. 4, pp. 8487–8499, 2016.
[24] P. Liu, L. Xiao, and T. Li, "A variational pan-sharpening method based on spatial fractional-order geometry and spectral-spatial low-rank priors," *IEEE Trans. Geosci. Remote Sens.*, vol. 56, no. 3, pp. 1788–1802, Mar. 2018.
[25] I. Zachevsky and Y. Y. J. Zeevi, "Statistics of natural stochastic textures and their application in image denoising," *IEEE Trans. Image Process.*, vol. 25, no. 5, pp. 2130–2145, May 2016.
[26] H. Lv, Z. Wang, S. Fu, C. Zhang, L. Zhai, and X. Liu, "A robust active contour segmentation based on fractional-order differentiation and fuzzy energy," *IEEE Access*, vol. 5, pp. 7753–7761, 2017.
[27] Y.-F. Pu, J.-L. Zhou, and X. Yuan, "Fractional differential mask: A fractional differential-based approach for multiscale texture enhancement," *IEEE Trans. Image Process.*, vol. 19, no. 2, pp. 491–511, Feb. 2010.
[28] T. Cao, W. Wang, S. Tighe, and S. Wang, "Crack image detection based on fractional differential and fractal dimension," *IET Comput. Vis.*, vol. 13, no. 1, pp. 79–85, Feb. 2019.
[29] X. Yang and B. Guo, "Fractional-order tensor regularisation for image inpainting," *IET Image Process.*, vol. 11, no. 9, pp. 734–745, Sep. 2017.
[30] Y.-F. Pu, "Fractional-order Euler-Lagrange equation for fractional-order variational method: A necessary condition for fractional-order fixed boundary optimization problems in signal processing and image processing," *IEEE Access*, vol. 4, pp. 10110–10135, 2016.
[31] J. Yu, L. Tan, S. Zhou, L. Wang, and M. A. Siddique, "Image denoising algorithm based on entropy and adaptive fractional order calculus operator," *IEEE Access*, vol. 5, pp. 12275–12285, 2017.
[32] Y.-F. Pu, P. Siarry, A. Chatterjee, Z.-N. Wang, Z. Yi, Y.-G. Liu, J.-L. Zhou, and Y. Wang, "A fractional-order variational framework for retinex: Fractional-order partial differential equation-based formulation for multi-scale nonlocal contrast enhancement with texture preserving," *IEEE Trans. Image Process.*, vol. 27, no. 3, pp. 1214–1229, Mar. 2018.

CHUNBO XIU received the Ph.D. degree in navigation, guidance, and control from the Beijing Institute of Technology, Beijing, China, in 2005. He is currently a Professor with the School of Electrical Engineering and Automation, Tianjin Polytechnic University, China. His research interests include neural networks, system modeling, and chaos control.

XIN LI received the B.S. degree in control science and engineering from the Tianjin University of Technology and Education, Tianjin, China, in 2017. She is currently pursuing the M.S. degree with the School of Electrical Engineering and Automation, Tianjin Polytechnic University, China. Her research interests include neural networks and image processing.